



Gioia, M., Fasciglione, G. F., Sbardella, D., Sciandra, F., Casella, M., Camerini, S., Crescenzi, M., Gori, A., Tarantino, U., Cozza, P., Brancaccio, A., Coletta, M., & Bozzi, M. (2018). The enzymatic processing of α -dystroglycan by MMP-2 is controlled by two anchoring sites distinct from the active site. *PLoS ONE*, 13(2), e0192651. <https://doi.org/10.1371/journal.pone.0192651>

Publisher's PDF, also known as Version of record

License (if available):
CC BY

Link to published version (if available):
[10.1371/journal.pone.0192651](https://doi.org/10.1371/journal.pone.0192651)

[Link to publication record in Explore Bristol Research](#)
PDF-document

University of Bristol - Explore Bristol Research

General rights

This document is made available in accordance with publisher policies. Please cite only the published version using the reference above. Full terms of use are available:
<http://www.bristol.ac.uk/red/research-policy/pure/user-guides/ebr-terms/>

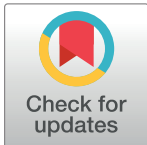
RESEARCH ARTICLE

The enzymatic processing of α -dystroglycan by MMP-2 is controlled by two anchoring sites distinct from the active site

Magda Gioia^{1,2*}, Giovanni Francesco Fasciglione^{1,2}, Diego Sbardella^{1,2}, Francesca Sciandra³, MariaLuisa Casella⁴, Serena Camerini⁴, Marco Crescenzi⁴, Alessandro Gori⁵, Umberto Tarantino¹, Paola Cozza¹, Andrea Brancaccio^{3,6}, Massimo Coletta^{1,2}, Manuela Bozzi^{3,7*}

1 Department of Clinical Sciences and Translational Medicine, University of Roma Tor Vergata, Roma, Italy, **2** CIRCMSB, Bari, Italy, **3** CNR Institute for Molecular Recognition, Roma Italy, **4** Istituto Superiore di Sanità, Roma, Italy, **5** CNR Institute for Molecular Recognition, Milano Italy, **6** School of Biochemistry, University of Bristol, Bristol, United Kingdom, **7** Institute of Biochemistry and Clinical Biochemistry, Catholic University, Roma Italy

* magda.gioia@uniroma2.it (MG); manuela.bozzi@unicatt.it (MB)



Abstract

Dystroglycan (DG) is a membrane receptor, belonging to the dystrophin-glycoprotein complex (DGC) and formed by two subunits, α -dystroglycan (α -DG) and β -dystroglycan (β -DG). The C-terminal domain of α -DG and the N-terminal extracellular domain of β -DG are connected, providing a link between the extracellular matrix and the cytosol. Under pathological conditions, such as cancer and muscular dystrophies, DG may be the target of metalloproteinases MMP-2 and MMP-9, contributing to disease progression. Previously, we reported that the C-terminal domain α -DG (483–628) domain is particularly susceptible to the catalytic activity of MMP-2; here we show that the α -DG 621–628 region is required to carry out its complete digestion, suggesting that this portion may represent a MMP-2 anchoring site. Following this observation, we synthesized an α -DG based-peptide, spanning the (613–651) C-terminal region. The analysis of the kinetic and thermodynamic parameters of the whole and the isolated catalytic domain of MMP-2 (cdMMP-2) has shown its inhibitory properties, indicating the presence of (at least) two binding sites for the peptide, both located within the catalytic domain, only one of the two being topologically distinct from the catalytic active groove. However, the different behavior between whole MMP-2 and cdMMP-2 envisages the occurrence of an additional binding site for the peptide on the hemopexin-like domain of MMP-2. Interestingly, mass spectrometry analysis has shown that α -DG (613–651) peptide is cleavable even though it is a very poor substrate of MMP-2, a feature that renders this molecule a promising template for developing a selective MMP-2 inhibitor.

OPEN ACCESS

Citation: Gioia M, Fasciglione GF, Sbardella D, Sciandra F, Casella M, Camerini S, et al. (2018) The enzymatic processing of α -dystroglycan by MMP-2 is controlled by two anchoring sites distinct from the active site. PLoS ONE 13(2): e0192651. <https://doi.org/10.1371/journal.pone.0192651>

Editor: Israel Silman, Weizmann Institute of Science, ISRAEL

Received: October 31, 2017

Accepted: January 26, 2018

Published: February 15, 2018

Copyright: © 2018 Gioia et al. This is an open access article distributed under the terms of the [Creative Commons Attribution License](https://creativecommons.org/licenses/by/4.0/), which permits unrestricted use, distribution, and reproduction in any medium, provided the original author and source are credited.

Data Availability Statement: All data are within the paper.

Funding: This work has been supported by funds from the Italian Space Agency (ASI SMEMCO n. DC-DTE-2011-033 to U.T.).

Competing interests: The authors have declared that no competing interests exist.

Introduction

Dystroglycan (DG) is a membrane receptor belonging to the dystrophin-glycoprotein complex (DGC). DG is formed by two subunits, alpha-dystroglycan (α -DG) and beta-dystroglycan (β -DG), that provide a link between the extracellular matrix and the cytoskeleton [1]. α -DG is a highly glycosylated extracellular protein that interacts with laminin, agrin and other extracellular proteins [2, 3], whereas β -DG is a transmembrane protein, associated with actin through dystrophin [4]. Inside the cell, β -DG is involved in a network of interactions with many proteins, including some factors belonging to different signaling pathways [5, 6]. The two subunits are held together by non-covalent interactions occurring between the C-terminal domain of α -DG and the extracellular N-terminal domain of β -DG [7]. These interactions play a crucial role for the integrity of the entire DGC [8], that is in turn responsible for the stability of the plasma membrane, especially in the skeletal muscle and in the central nervous system, where DG is mainly expressed [9]. Under pathological conditions, such as cancer and neuromuscular diseases (including severe muscular dystrophies) [10], disruption of the DG subunits is often associated to the over-expression of some members of the metalloproteinase (MMP) family [11–15], which are Zn^{2+} -dependent endopeptidases critical for tissue homeostasis and cell signaling [16, 17]. The structural modular architecture of MMP family shows (from N-terminus to C-terminus) a propeptide domain, which is removed upon enzyme activation, a catalytic domain and a hemopexin-like domain, which are connected by a hinge region [18]. The isolated catalytic domain of all MMP members retains the capability of cleaving linear peptidic substrates according to the specific substrate selectivity of each single subclass of the family [19]. Importantly, MMP gelatinases, namely MMP-2 and MMP-9, possess a unique additional collagen binding domain (CBD), inserted within the MMP's catalytic domain sequence [20]. The peculiarity of the CBD domain concerns its involvement in the recognition and binding of protein substrates, a role exerted prevalently by the hemopexin-like domain in other MMPs, providing an ancillary binding surface which governs the cleavage specificity of very complex macromolecular substrates, such as 3D triple helical collagens [21–26].

Many physiological substrates for MMPs, including membrane proteins, are shed from the cell surface, often showing distinct biological functions in the proteolyzed form [19, 27, 28]. In particular, MMP gelatinases remove the extracellular N-terminal domain of β -DG, producing a 30 kDa truncated form of β -DG [11, 29, 30]. Two molecular mechanisms, differing between the two gelatinases, have been described *in vitro* for the shedding of the β -DG N-terminal domain. Thus, MMP-9 operates the first cleavage, removing at the N-terminal region of about 60 amino acids, which is further degraded, and leaving an intact C-terminal fragment of about 30 amino acids [31]; on the other hand, MMP-2 completely disrupts the β -DG N-terminal domain, producing multiple cleavages [32]. *In vivo*, disruption of the β -DG N-terminal domain is likely to leave the C-terminal domain of α -DG exposed to a variety of endopeptidases, that exert their catalytic activity within the extracellular matrix. However, recent findings report that double-targeting of MMP-2 and MMP-9 cannot prevent cleavage of β -DG in sarcoglycanopathy [33]. Processing and secretion of N-terminal domain of α -DG in cell culture media has been previously reported [34]. Further, *in vitro* we have revealed that native α -DG can be degraded by MMP-2, with the α -DG C-terminal domain representing the region most susceptible to the protease activity [35]. Computational analysis on all MMP cleavage sites reported in literature showed that MMPs cleave preferentially in exposed loops and in disordered regions of proteins [36]. No structural information is available for the α -DG C-terminal domain, but a modeling study suggested the presence of an Ig-like domain for the region approximately comprised between amino acids 500–600, followed by a coil-helix-coil motif spanning the amino acids 601–651 [37]. *In vitro*, the recombinant α -DG C-terminal domain

can be degraded by MMP-2, whereas a shorter co-purified α -DG-fragment is fully resistant to the enzyme, suggesting the presence of a MMP-2 recognition site involving the missing amino acids [35]. In this work, we have assigned by mass spectrometry the sequence of this shorter fragment as α -DG (483–621), and we focused our investigation on the full C-term construct α -DG (483–628), following its proteolysis kinetics by MMP-2. Overall, we confirmed the proposed mechanism and showed that a peptide, spanning the last 39 amino acids of the α -DG C-terminus, namely α -DG (613–651) peptide, can modulate (already within the nanomolar range of concentrations) the MMP-2 catalysis of the entire enzyme and of its isolated catalytic domain (cdMMP-2).

Materials and methods

Materials

The purity of Human recombinant MMP-2 of whole proenzymes (R&D System, London, UK) and its catalytic domain cdMMP-2 (Biomol International) was measured by sodium dodecyl sulfate (SDS) polyacrylamide gel electrophoresis (PAGE) according to the Laemmli's method. After the gels had been run, they were stained using a silver staining kit (Bio-Rad, Hercules, CA, USA). The broad spectrum protein markers (Bio-Rad, Hercules, CA, USA) were used as molecular weight standards. The stability of MMP-2 was checked by zymography (employing as the substrate either gelatin or type I collagen) [38]. The MMP-2 is perfectly stable (without undergoing any autocatalytic activity in the presence of the α -DG solution at 37°C) for well over 60 min, which covers by far the time period needed for the measurements of the catalytic parameters (*i.e.*, 15 minutes).

p-Hydroxybenzyl alcohol resin (Wang) and *N*- α -Fmoc-L-amino acids used during chain assembly were purchased from Iris Biotech GmbH (Marktredwitz, Germany). [2-(1*H*-benzotriazol-1-yl)-1,1,3,3-tetramethyluronium hexafluorophosphate] (HBTU) was purchased from Fluka (Buchs, Switzerland), *N,N'*-dimethylformamide (DMF) and trifluoroacetic acid (TFA) were from Carlo Erba (Rodano, Italy). *N,N'*-diisopropylethylamine (DIEA), dichloromethane (DCM), triisopropylsilane (TIPS), *N*-methyl pyrrolidone (NMP) and all other organic reagents and solvents, unless stated otherwise, were purchased in high purity from Sigma-Aldrich (Steinheim, Germany). All solvents for solid-phase peptide synthesis (SPPS) were used without further purification. HPLC grade acetonitrile and ultrapure 18.2 Ω water (MilliQ) were used for the preparation of all solvents for liquid chromatography.

DNA manipulation

The full-length cDNA encoding for murine DG was used as a template to generate by PCR two DNA construct corresponding to the C-terminal region of α -DG, α -DG(483–628). Appropriate primers were used to amplify the DNA sequence of α -DG(483–628): forward 5' -CCC**GTGAC**AGTGGAGTGCCCCGTGGGGGAGAAC-3' and reverse 5' -CCC**GAATTC**TTATACCAAAGCAATTTTCTTGTGAATG-3' , *Sall* and *EcoRI* restriction sites are in bold type.

Protein expression and purification

The DNA construct obtained was purified and cloned into a bacterial vector which is appropriate to express the protein as thioredoxin fusion product, also containing an N-terminal 6His tag and a thrombin cleavage site. The recombinant fusion protein was expressed in *Escherichia coli* BL21(DE3) Codon Plus RIL strain (Agilent Technologies, Australia), since no glycosylation sites have been found in the native eukaryotic protein [39], and purified using

nickel affinity chromatography. The construct of interest was obtained upon thrombin cleavage. Tricine/SDS-PAGE was used to check the purity of the recombinant proteins under analysis.

Chemical synthesis and purification of the C-term peptide

Linear peptide was assembled on a Wang resin (0.6 mmol/g) in a 0.10 mmol scale. Resin was properly swelled prior use with a NMP/DCM mixture. Peptide assembling was performed automatically on a Biotage ALSTRA peptide synthesizer using a Fmoc-chemistry protocol. Coupling of entering Fmoc-protected amino acids was performed using HBTU/DIEA (1:1:2, 4 equivalents excess over resin loading, 1 x 5min, 75°C). Deprotection steps were performed by treatment with a 20% piperidine solution in DMF (2x5min, RT). Following each coupling or deprotection step, resin-bound peptide was washed 5 times with DMF. Following chain assembly, peptides were cleaved from the resin using a TFA 90%, Water 5%, Phenol 2.5%, TIPS 2.5% mixture (2 hours, RT). Following precipitation in cold diethyl ether, crude peptides were collected by centrifugation and subsequently washed with further cold diethyl ether to remove scavengers. Peptides were then dissolved in a 50% aqueous acetonitrile 0.07% TFA buffer and underwent RP-HPLC purification.

Analytical and semi-preparative Reversed Phase High Performance Liquid Chromatography (RP-HPLC) were carried out on a Tri Rotar-VI HPLC system equipped with a MD-910 multichannel detector for analytical purposes or with a Uvidec-100-VI variable UV detector for preparative purpose (all from JASCO, Tokyo, Japan). A Phenomenex Jupiter 5 μ C18 90Å column (150 x 4.6 mm) was used for analytical runs and a Phenomenex Jupiter 10 μ C18 90Å (250 x 21.2 mm) for peptide purification. Data were recorded and processed with Borwin software. A linear gradient of eluent B (eluent A = H₂O/ 3% CH₃CN / 0.07% TFA, eluent B = 70% CH₃CN/ 30% H₂O/ 0.07% TFA) was employed at a flow rate of 1 mL/min for analytic purposes. UV detection was recorded in the 220–320 nm range. Purification of the peptides was achieved by preparative RP-HPLC at a flow rate of 14 mL/min using a linear gradient of eluent B. Pure RP-HPLC fractions (>95%) were combined and lyophilized. Mass spectra were collected separately.

Mass spectrometry analysis of the recombinant α -DG(483–628) domain and of the α -DG(613–651) peptide

Recombinant α -DG (483–628) domain was separated on 1D-gel NuPAGE 4–12% (Novex, Invitrogen) and stained with the Colloidal Blue Staining kit (Invitrogen). The stained bands were cut, incubated with 10 mM DTT for 1h at 56°C, then with 50 mM iodoacetamide for 45min at RT in the dark, subsequently dried before enzymatic digestion that was performed with 12.5 ng/ml LysC or GluC (Roche) at 37°C over night.

Samples containing the (613–651) peptide were cleaned by 30kDa cutoff filters to remove MMP-2 and desalted by C18 Zip Tip (Millipore) before mass spectrometry analysis. Peptide mixture deriving from the enzymatic reactions (α -DG (483–628) domain treated with LysC, GluC or (613–651) peptide incubated with MMP2) were analyzed by nanoflow-reversed-phase liquid chromatography tandem mass spectrometry (RP-LC-MS/MS) using an HPLC Ultimate 3000 (DIONEX, Sunnyvale, CA U.S.A) connected on line with a linear Ion Trap (LTQ, Thermo, San Jose, CA). Peptides were desalted in a trap-column (AcclaimPepMap100 C18, LC Packings, DIONEX) and then separated in a 10 cm long fused silica capillary (SilicaTipsFS 360-75-8, New Objective, Woburn, MA, USA), slurry-packed in-house with 5 μ m, 200 Å pore size C18 resin (Michrom BioResources, CA). Peptides were eluted using a 45 min long linear gradient from 20% to 50% acetonitrile in presence of 0.1% formic acid at 300 nl/min flow rate,

followed by 50 min during which the column was washed and then equilibrated again. Spectra were acquired in positive ion mode (HV Potential 1.7–1.8kV) in a data-dependent mode: each full MS spectrum was followed by the fragmentation of the five most abundant precursor ions. MS/MS spectra were analyzed using the Proteome Discoverer 1.4 software (Thermo) and database from Swiss-Prot containing *E. coli* proteins and / or α -DG sequence.

Enzymatic assays

Human MMP-2 proenzyme 2 was activated by incubating 0.1 mg/ml progelatinase solution with 0.25 mM aminophenyl mercuric acid (Sigma, St. Louis, MO, USA) at 37°C for 30 minutes. Whereas human recombinant cdMMP-2 human was dissolved in a solution of 50 mM Tris/HCl (pH 7.2), 0.1M NaCl and 10 mM CaCl₂. The actual concentration of active MMP-2 (i.e. whole MMP2 and cdMMP2) was determined by the classic fluorimetric assay [38], following the progressive decrease of hydrolysis (upon addition of an irreversible inhibitor, ilomastat (GM 6001) which stoichiometrically inhibits MMPs) of the MCA- Pro-Leu-Gly-Leu-DPA-Ala-Arg-NH₂ fluorogenic substrate (λ_{exc} = 325 nm, λ_{em} = 398 nm). All measurements were performed at 37°C using a solution of 50 mM Tris-HCl, 0.1 M NaCl, 10 mM CaCl₂ and 0.05% Brij 35 buffered at pH 7.3.

α -DG domain degradation assay

The α -DG domain degradation by MMP-2 was performed in 50 mM Tris-HCl, 0.1 M NaCl, 10 mM CaCl₂ the mixtures were kept at 37°C and small aliquots were harvested at different time intervals (ranging from 0 and 18 hours). The reactions were stopped by the addition of SDS-PAGE loading buffer containing 20 mM EDTA, boiled for 2 minutes and frozen to -80°C until they were used.

Equal aliquots from the incubation mixtures were collected at increasing times, the samples were separated on gradient precast TRIS glycine 10–20% SDS-PAGE gels and these were stained using 0.5% Coomassie blue, followed by destaining until substrate bands were clearly visible. The Coomassie blue electrophoretic spots corresponding to each time intervals were analyzed by image analysis software (Image Quant TL, Amersham Biosciences). For the evaluation of pixel intensity, the pixel brightness through the region of interest was measured and plotted using Graphpad Prism v6 software. Histograms reported the relative amount intensity (expressed as arbitrary units and converted to percentage according to the ratio = band intensity at the starting point $t = 0$ / intensity at any given time interval). Data were presented as means \pm standard deviation of three independent experiments. The difference between the two groups was compared with one-way ANOVA followed by Tukey post-hoc test by GraphPad Prism, version 6.0 GraphPad software (La Jolla Ca), * $p < 0.05$ was considered significant.

Modulation of the α -DG C-terminal peptide on the MMP-2 activity

Different concentrations of the α -DG peptide (i.e., final concentration range spanning between 0 μ M and 4 μ M) were incubated with 0.07 μ M active MMP-2 for 30 min at 37°C to allow the interaction to occur. In the case of the cdMMP2 the kinetics were performed employing 0.06 μ M cdMMP-2 at different concentration of α -DG (613–651) peptide in the range 0–2 μ M. Different concentrations of MCA fluorogenic peptide (i.e: from 5 to 15 mM) were then added to this solution. The enzymatic reaction was recorded for 30 minutes at 37°C. The initial velocities were derived from the slopes within the first 15 minutes, which is the time period during which the rate is constant and less than 10% of the substrate was degraded. This ensured a steady-state condition for the first cleavage step, and it was a prerequisite for the subsequent analysis steps.

Results

Characterization of recombinant α -DG (483–628) domain by mass spectrometry

As already shown in our previous work [35], the murine α -DG C-term domain (construct expressed and purified in *E. coli*) displayed two electrophoretic bands: an upper band (~17 kDa) and a lower band (~15 kDa).

To verify the absence of contamination from *E. coli* and confirm the identity of the purified α -DG (483–628) domain, the two bands have been enzymatically *in gel*-digested and analyzed by LC-MS/MS. The analysis of both bands confirmed the presence of several peptides deriving from the α -DG (483–628) domain and no contaminant proteins from *E. coli* were detected. Moreover, whilst the peptide mixture from the upper band allowed to map the sequence until the leucine at position 627, as revealed by the (608–627) peptide (Table 1 and Fig 1), the enzymatic digestion of the lower band produced the (608–621) peptide (Table 1 and Fig 1), which is absent in the upper band. These data indeed suggest that the lower band is a degradation product which co-purifies with the recombinant α -DG (483–628) domain, likely ending with the isoleucine at position 621.

The α -DG (613–651) peptide inhibits MMP-2 processing of α -DG (483–628) domain

Degradation kinetics of 7 μ M α -DG (483–628) domain (see Fig 2) by 14 nM MMP-2 is analyzed by SDS-PAGE electrophoresis separation (Fig 2B, upper lanes). In line with our previous work [35], the intensity of the ~17 kDa electrophoresis band progressively reduces its intensity over time while, concurrently, the lower band (~15 kDa) is resistant to the MMP-2 proteolytic

Table 1. X Corr indicates cross-correlation score that is the sequet measure of the goodness of fit of experimental peptide fragments to theoretical spectra. Upper band and Lower band refer to the bands visible in the gel in the Fig 2. z is the peptide charge detected.

Position	Enzyme	Peptide sequence	Upper band		Lower Band	
			X Corr	z	X Corr	z
497–513	GluC	LKNHIDRVDAWVGTYFE	4.91	2	4.74	2
499–515	LysC	NHIDRVDAWVGTYFEVK	4.83	2	4.49	2
499–531	LysC	NHIDRVDAWVGTYFEVKIPSDTFYDNEDTTTDK	5.11	5	5.31	5
513–540	GluC	VKIPSDTFYDNEDTTTDKCLKLTLKLE	4.68	4	4.18	3
516–531	LysC	IPSDTFYDNEDTTTDK	3.7	2	3.44	2
516–533	LysC	IPSDTFYDNEDTTTDKCLK	4.49	4	3.85	3
516–537	LysC	IPSDTFYDNEDTTTDKCLKLTLK	3.99	5	4.5	3
532–547	LysC	LKLTCLKLREQQLVGEK	4.01	4	3.04	3
541–572	GluC	QQLVGEKSWVQFNSNSQLMYGLPDSSSHVGKHE	3.38	2	3.13	4
547–572	GluC	KSWVQFNSNSQLMYGLPDSSSHVGKHE	6.81	3	7.17	3
547–572	GluC	KSWVQFNSNSQLMYGLPDSSSHVGKHE	6.49	3	6.84	3
548–570	LysC	SWVQFNSNSQLMYGLPDSSSHVGK	5.32	3	5.06	3
548–570	LysC	SWVQFNSNSQLMYGLPDSSSHVGK	4.93	5	4.85	3
548–580	LysC	SWVQFNSNSQLMYGLPDSSSHVGKHEYFMHATDK	3.2	2	3.05	5
573–590	GluC	YFMHATDKGGLSAVDAFE	4.98	2	4.19	2
573–590	GluC	YFMHATDKGGLSAVDAFE	4.37	4	3.92	2
581–595	LysC	GGLSAVDAFEIHVHK	4.51	2	4.73	2
608–621	LysC	ARLAGDPAPVVNDI			3.75	2
608–627	LysC	ARLAGDPAPVVNDIHKIAL	4.65	2		

<https://doi.org/10.1371/journal.pone.0192651.t001>

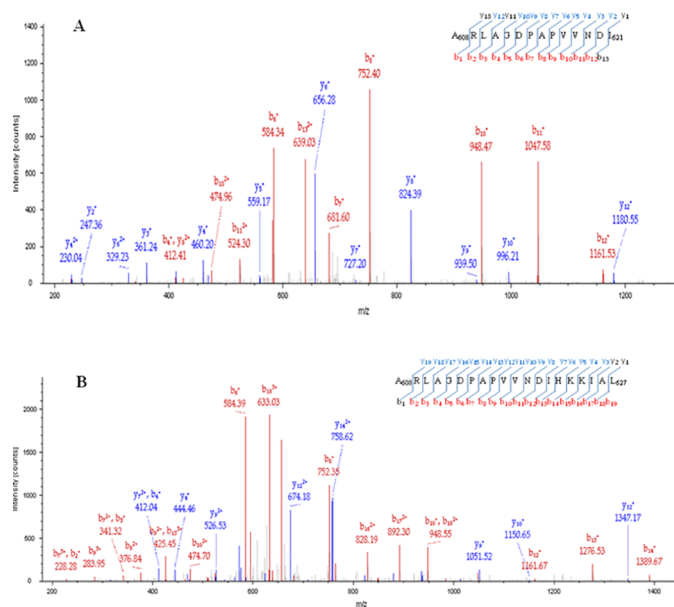


Fig 1. MS LC-MS/MS analysis of the purified α DG (483–628) domain. MS/MS spectra of the (608–621) peptide (A) and (608–627) peptide (B) deriving from LysC digestion of lower and upper band of the gel shown in Fig 2, respectively. Matched b and y ions are colored in red and blue, respectively.

<https://doi.org/10.1371/journal.pone.0192651.g001>

activity (Fig 2B, upper lanes). In order to unravel the role of the MMP-2 hemopexin-like domain for the differential fragmentation, the proteolysis kinetics of the α -DG (483–628) domain was also performed employing 30 nM of the isolated catalytic domain cdMMP-2. Fig 2C (upper lanes) shows that also the catalytic domain of MMP-2 (without the hemopexin-like domain) retains the capability of degrading the α -DG (483–628) domain, even though in this case the proteolytic cleavage of the α -DG domain appears less specific, the degradation occurring both on the 17 kDa band and the 15 kDa band (Fig 2C, upper lanes). Therefore, the data reported in Fig 2 clearly indicate that

1. the cleavage of the α -DG (483–628) domain by MMP-2 does not require the presence of the hemopexin-like domain, since also cdMMP-2 enzymatically processes this domain;
2. the hemopexin-like domain likely plays a functional regulatory role by addressing MMP-2 toward a specific binding site, located within the C-terminal region between amino acid positions 621–628, thus avoiding unspecific and widespread fragmentation of the all macromolecular substrate.
3. The presence of the hemopexin-like domain in the whole MMP-2 protects the α -DG 483–621 domain from the enzymatic processing.

Therefore, the hemopexin-like domain, though not required for the cleavage of the α -DG (483–628) domain, is nonetheless crucial for proper substrate positioning of MMP-2, envisaging its interaction with the 621–628 amino acid region.

In order to cast some light on the role of the 621–628 amino acid region on the α -DG processing, we have chemically synthesized a human α -DG (613–651) peptide which shares a closely similar amino acid sequence with murine α -DG 611–649 (see Fig 3). Therefore, we have investigated the functional effect of the α -DG (613–651) peptide on the enzymatic processing by MMP-2 of the α -DG (483–628) domain.

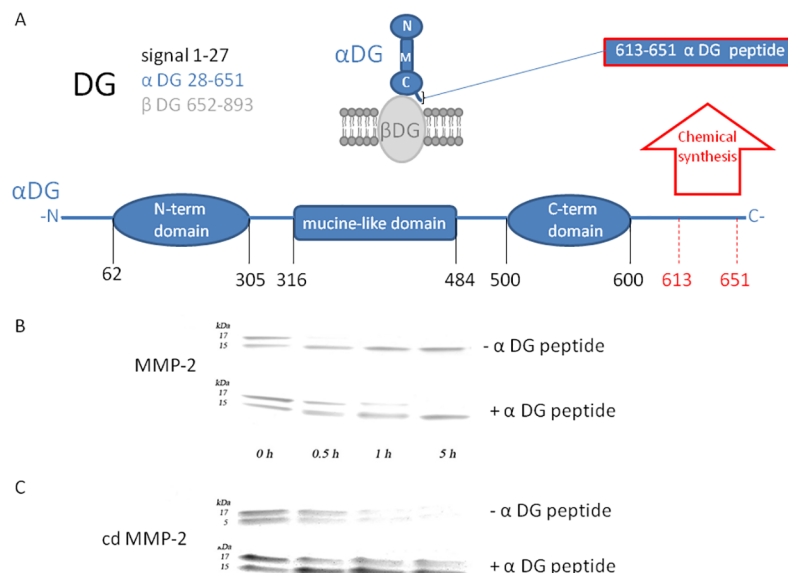


Fig 2. The α DG (613–651) peptide affects the degradation of α DG (483–628) peptide (Panel A) Aminoacidic sequences associated with each subunits of murine DG and its schematic representation. Enzymatic proteolysis profiles of the purified α -DG C-terminal domain (483–628) construct by MMP-2 (Panel B), or by cdMMP-2 (Panel C) are represented by the sodium dodecyl sulfate polyacrylamide gels stained with Coomassie blue. Four-point time course was represented: time 0, time 30 s, time 1 hour, time 5 hours in the absence (upper panel) and in the presence (lower panel) of 4 μ M of the α -DG (613–651) peptide. Equal aliquots from the incubation mixtures were collected at increasing times, the reaction was stopped and samples were separated by TRIS glycine 10–20% precast gel.

<https://doi.org/10.1371/journal.pone.0192651.g002>

Under the same experimental conditions, the degradation rate of the α -DG (483–628) domain was much slower in the presence of 4 μ M of α -DG peptide (Fig 2). Indeed, a significant decrease of the 17 kDa band could be observed only after 5 hours of MMP-2 activity (Fig 2A, lower lanes) and a similar inhibitory effect was also detected in the case of cdMMP-2 (Fig 2B, lower lanes); furthermore, in the case of cdMMP-2, the presence of the α -DG (613–651) peptide appears to inhibit even the enzymatic processing of the 15 kDa band (Fig 2B, lower lanes). This feature suggests that the inhibitory effect is exerted through a direct binding of the α -DG (613–651) peptide on cdMMP-2. This interaction not only interferes with the proteolytic cleavage of the α -DG (613–651) sequence, but it also impairs the interaction of cdMMP-2 with additional substrate exosites, which can explain the extended and widespread fragmentation of the shorter α -DG (483–621) domain in the absence of the peptide (Fig 2B, upper lanes).

The similar inhibitory behavior suggests that the binding site of the α -DG (613–651) peptide is located at the catalytic domain of MMP-2 and, given that the α -DG(483–628) domain partially overlaps with the α -DG(613–651) peptide, this result indicates also that the interaction of α -DG(483–628) domain with MMP-2 involves also the catalytic domain.

MMP-2 enzymatic activity toward a fluorogenic peptide is inhibited by the human α -DG C-term (613–651) peptide

In order to determine the inhibitory mechanism, exerted by the α -DG (613–651) peptide on MMP-2 and its cd-MMP-2, a small fluorogenic substrate (MCA-Pro-Leu-Gly-Leu-DPA-Ala-Arg-NH₂) was employed. Fig 4 reports the Lineweaver-Burk plots of the degradation kinetics of the fluorogenic substrate carried out by the whole MMP-2 in the presence of increasing amounts of the α -DG(613–651) peptide over a range of concentrations spanning between 0 and 4 μ M (Fig 4A and 4B). It immediately comes out that the inhibitory effect displays a

>sp|Q62165|DAG1_MOUSE Dystroglycan OS=Mus musculus GN=Dag1

```

10      20      30      40      50      60
MSVDNULHLP LUGQTFLLLL SVAVAQAHPW SEPSEAVRDW KNQLEASMS VLSDFEAVP
TVVGIPDGTAVVGRSFRVSIPTDLIASSGE IIKVSAAGKE ALPSWLHWDH HSHILEGLPL 120
DTDKGVHYISVSAARLGANGSHVPQTSSVF SIEVYPEDHN EPQSVRAASS DPGEVVPASAC 180
AADEPVTVLTVILDADLTGMTPKQIRIDLLN RMQSFSEVEL HNMKLVPPVN NRLEFMSAFM 240
AGPGNAKKVVENGALLSWKLGCSLNQNSVP DIRGVETPAR EGAMSAQLGY PVVGVHIANK 300
KPTLPKRLRRQIHATPTPTVAIGPPTTAIQ EPPSRIVPTP TSPAIAAPTE TMAPPVVRDPV 360
PGKPTVTIIRTGAIITQPTL GPIQPTRVSE AGTTVPQGIR PTLTIPGYVE PTAVITPPTT 420
TTKKPRVSTPKPATPSTDSS TTTTTRRPTTK PRTPRPVPRV TTKAPITRLE TASPPTRIRT 480
TTSQVPRGGE PNQRPELKNH IDRVDHVGTYFEVKIPSDT FYDNEDTTD KLKLTLKLE 540
QQLVGEKSWVQENSNSQLMYGLPDSSHVGK HEYFMHATDK GGLSAVDAFE IHWKRPQGD 600
KAPARFKAAGDPAPVVDNIHKKIALVKK LAFAGDRNC SSITLQNIIRGSIVVEVTNN 660
TLPLEPCPKQIIGLSRRIDENGGKPPAF SNALEPDFKA LSIATVGSGL CRHLQIPVA 720
PPSPGSSAAPATEVPDRDPEKSSDDVYLHTVIPAVVVAAILLIAGIIMICYRKKRKGK 780
LTLEDQATFIKKGVPPIFAD ELDDSKPPSPSSMPLILQEEKAPLPPEYPNQSPETTPPL 840
NQDVTGVEYTPLRDEDPNAPYQPPPPFTAPMEGKSRPKNMTFYRSPPPYVPP

```

483-628

611-649

A₆₁₁GDPAVVDNIHKKIALV₆₂₈

>sp|Q14118|DAG1_HUMAN Dystroglycan OS=Homo sapiens GN=DAG1

```

10      20      30      40      50      60
MRMSVGLSLL LPLSGRTFLL LLSVMAQSHWPSEPSEAVRDWENQLEASHSVLSDLHEA
VPTVVGIPDGTAUVGRSFRVSIPTDLIASSGDIKVSAAAGKEALPSWLHWDHDSQSHLEGL 120
PLDTDKGVHYISVSATRLGANGSHIPQTSSVFSIEVYPEDHSELQSVRTASPDGEVVSS 180
ACAADPEVTVLTVILDADLTGMTPKQIRIDLLNRMRSFSEVELHNMKLVPPVNNRLEFMSA 240
FMAGPGNAKKVVENGALLSWKLGCSLNQNSVPDIRHGVETPAR EGAMSAQLGYPVVGVHIA 300
NKKPLPKRVRRQIHATPTPTVAIGPPTTAIQEPPSRIVPTTSPAIAAPTE TMAPPVVRDPV 360
PVPKPTVTIIRTGAIITQPTL GPIQPTRVSEAGTTVPQGIRPTMTIPGYVEPTAVATPP 420
TTTTKKPRVSTPKPATPSTD TTTTTRRPTTKPRTPRPVPRV RVTTKVSITRLETASPPTRI 480
RTTTSQVPRGGE PNQRPELKNH IDRVDHVGTYFEVKIPSDT FYDNEDTTD KLKLTLKLE 540
REQQLVGEKSWVQENSNSQLMYGLPDSSHVGKHEYFMHATDKGGLSAVDAFEIHWKRPQGD 600
GDRAPARFKAAGDPAPVVDNIHKKIALVKKLAFAGDRNC SSITLQNIIRGSIVVEVTNN 660
NNTLPLEPCPKQIIGLSRRIDENGGKPPAF SNALEPDFKA LSIATVGSGL CRHLQIPVA 720
VPPRRVPSAPTEVPDRDPEKSSDDVYLHTVIPAVVVAAILLIAGIIMICYRKKRKGK 780
GKLTLEDQATFIKKGVPPIFAD ELDDSKPPSPSSMPLILQEEKAPLPPEYPNQSPETTPPL 840
PLNQDVTGVEYTPLRDEDPNAPYQPPPPFTAPMEGKSRPKNMTFYRSPPPYVPP

```

485-630

613-651

V₆₁₃GD₆₁₅PALVLDNIHKKIALV₆₃₀

Fig 3. Comparison between the amino acid sequence of murine (upper panel) and human (lower panel) DG (according to Swiss-Prot database). Amino acid sequences for signal peptides are in gray, for α -DG in bold, and for α -DG in brown. Amino acid sequence of murine α -DG(483–628) are in bold green (upper panel) while the corresponding sequence of human α -DG(485–630) is in bold blue. The amino acid sequence of the peptide derived from the C-terminal portion of human α -DG (in the highlighted red rectangle), contains the sequence (613–630) that overlaps with the corresponding mouse α -DG sequence (611–628), except for amino acids in light blue in the red rectangle in lower panel.

<https://doi.org/10.1371/journal.pone.0192651.g003>

bimodal behavior, since at lower concentrations (*i.e.*, between 23 nM and 0.4 μ M) a non-competitive mechanism seems operative (see Fig 4A), while at higher concentrations a competitive inhibition comes into play (see Fig 4B). Such a bimodal behavior can be observed also in Fig 4C and 4D, which represents the Lineweaver-Burk plots of the degradation kinetics of the fluorogenic substrate carried out by cdMMP-2 in the presence of increasing amounts of the α -

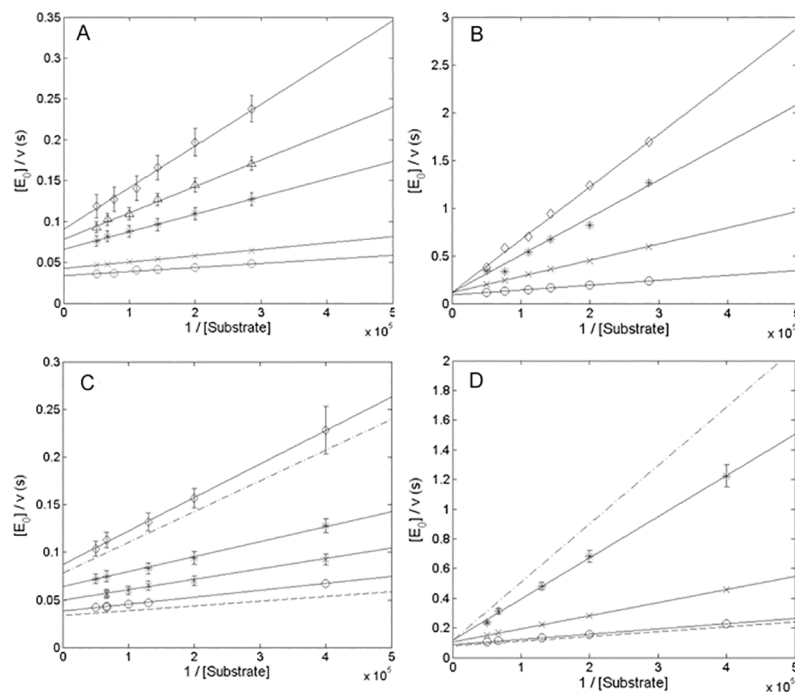


Fig 4. The effect of α DG (613–651) peptide on the catalytic parameters for the MMP-2 proteolysis. Lineweaver-Burk plot of the enzymatic activity of 60 nM MMP-2 at 37°C at pH 7.3 as a function of the fluorogenic substrate concentration at different concentrations of α -DG(613–651) peptide, namely (*panel A*) 0 (o), 23 nM (x), 125 nM (*), 200 nM (Δ) and 0.4 μ M (25CA), and (*panel B*) 0.4 μ M (o), 1 μ M (x), 2 μ M (*) and 4 μ M (\diamond). Continuous lines have been obtained by applying Eqs. (1)–(3), employing parameters reported in Table 2. (*Panel C*): namely 0 (o), 23 nM (x), 60 nM (*) and 0.2 μ M (\diamond), and, (*panel D*) 0.2 μ M (o), 0.6 μ M (x) and 2 μ M (*), and, (*panel D*) 0.2 μ M (o), 0.6 μ M (x) and 2 μ M (*). Continuous lines have been obtained by applying Eqs. (1)–(3), employing parameters reported in Table 2. Dashed line corresponds to the Lineweaver-Burk plot of the enzymatic activity of whole MMP-2 in the absence. Dashed-dotted lines corresponds to the Lineweaver-Burk plot in the presence of the α -DG(613–651) peptide 0.2 μ M and 2 μ M α -DG(613–651) peptide in *panel C* and *panel D*, respectively. Where not shown, standard deviation is smaller than symbol.

<https://doi.org/10.1371/journal.pone.0192651.g004>

DG(613–651) peptide, whose concentration values ranged between 0 and 2 μ M (Fig 4C and 4D).

This behavior, which envisages the presence of (at least) two binding sites for the α -DG (613–651) peptide on the catalytic domain of MMP-2, can be kinetically and thermodynamically described by the scheme reported on Fig 5; where, $^0k_{cat}$ and 0K_m are the observed catalytic parameters in the absence of the peptide, K_a and K_b are the peptide dissociation constants to the free enzyme for the two binding sites, α is the interaction parameter, which quantifies the effect on K_m of the α -DG(613–651) peptide binding to the first binding site ($\alpha > 1$ indicates a negative effect with a decreased affinity, $\alpha < 1$ a positive effect and $\alpha = 1$ no effect), β is the interaction parameter which estimates the effect on k_{cat} of the binding of α -DG(613–651) peptide to the first binding site ($\beta > 1$ indicates a positive effect with an increased rate constant, $\beta < 1$ a negative effect and $\beta = 1$ no effect).

Data reported in Figs 4 and 5 have been analyzed according to the following equation:

$$\frac{[E_0]}{v} = \frac{^{obs}K_m}{^{obs}k_{cat}} \cdot \frac{1}{[S]} + \frac{1}{^{obs}k_{cat}} \quad (\text{Eq 1})$$

where $[E_0]$ is the total enzyme concentration, v is the observed velocity (expressed as mol/s), $[S]$ is the substrate concentration, $^{obs}k_{cat}$ and $^{obs}K_m$ are the observed catalytic parameters,

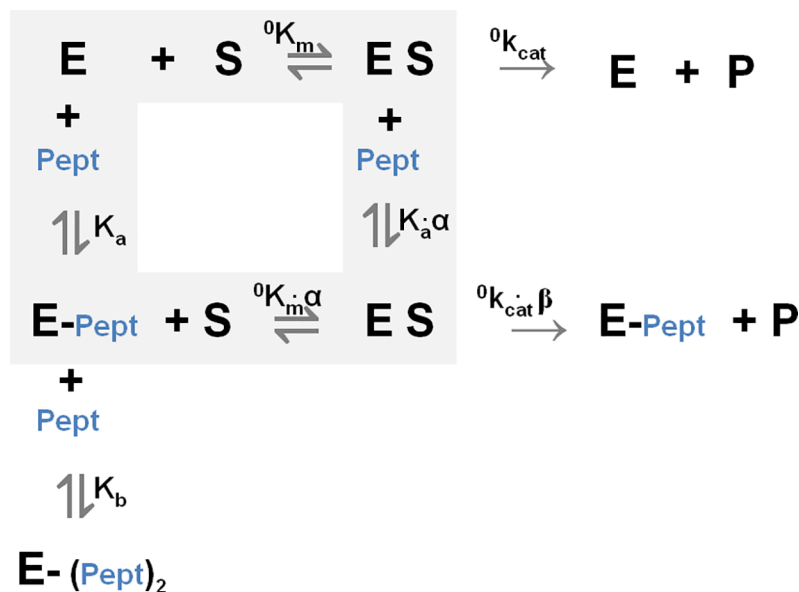


Fig 5. Thermodynamic and kinetic scheme for the effect of the α DG(613–651) peptide on the catalytic processing of the fluorogenic peptide. Where, pept represents the α DG(613–651) peptide, $^0k_{cat}$ and 0K_m are the observed catalytic parameters in the absence of the peptide, K_a and K_b are the peptide dissociation constants to the free enzyme for the two binding sites, α and β are the interaction parameters.

<https://doi.org/10.1371/journal.pone.0192651.g005>

namely

$$^{obs}k_{cat} = ^0k_{cat} \cdot \frac{(K_a \cdot \alpha + \beta \cdot [Pept])}{(K_a \cdot \alpha + [Pept])} \quad (\text{Eq 2})$$

and

$$^{obs}K_m = ^0K_m \cdot \frac{\alpha \cdot (K_a \cdot K_b + K_b \cdot [Pept] + [Pept]^2)}{K_b \cdot (K_a \cdot \alpha + [Pept])} \quad (\text{Eq 3})$$

where $^0k_{cat}$ and 0K_m are the catalytic parameters in the absence of peptide and all other symbols have the same meaning as described above.

The global fitting of data, reported in Fig 4, employing simultaneously Eqs (1), (2) and (3), allowed to obtain all parameters reported in Table 2. The peptide concentration dependence of catalytic parameters (k_{cat} and K_m) for both MMP-2 and cdMMP-2 confirms the appropriateness of the scheme adopted (Figs 5 and 6, see Table 2). It is interesting to observe as the peptide high affinity site for MMP-2 appears to be topologically distinct from the active site, envisaging

Table 2. All parameters from scheme employed for the description of the modulatory effect by the α -DG C-term peptide on the enzymatic activity of MMP-2 at pH 7.3 and 37°C for the fluorogenic substrate (see Fig 5).

	whole MMP-2	cd-MMP-2
$^0k_{cat} \text{ (s}^{-1}\text{)}$	29.6±4.5	26.1±4.1
$^0K_m \text{ (M)}$	1.5(±0.3)×10 ⁻⁶	1.9(±0.5)×10 ⁻⁶
$K_a \text{ (M)}$	3.5(±0.5)×10 ⁻⁸	3.5(±0.5)×10 ⁻⁸
$K_b \text{ (M)}$	2.1(±0.4)×10 ⁻⁷	2.1(±0.4)×10 ⁻⁷
α	1.7±0.4	1.25±0.25
β	0.27±0.04	0.32±0.05

<https://doi.org/10.1371/journal.pone.0192651.t002>

an allosteric modulation elicited by the α -DG (613–651) peptide on MMP-2, which reduces its enzymatic activity through both a decrease of substrate affinity for the catalytic center (as from $\alpha = 1.7 \pm 0.4$, see Table 2 and Fig 6B) and a slowing down of the rate-limiting step along the pathway of the substrate proteolytic cleavage (as from $\beta = 0.27 \pm 0.04$, see Table 2 and Fig 6A). Further addition of peptide enables its interaction with MMP-2 active site cleft, thereby exerting a competitive inhibition of the substrate enzymatic processing, as indicated by the lack of an effect on k_{cat} (see Figs 4B, 4D and 6A).

It can be observed that the catalytic parameters for the fluorogenic substrate are closely similar (within the experimental errors) between the whole MMP-2 and cdMMP-2 (see Table 2 and Figs 4 and 6). The comparison between the inhibitory mechanism of the peptide operating on the whole MMP-2 and on the cdMMP-2 reveals that for both species the α -DG (613–651) peptide binding sites are located at the catalytic domain and apparently share the same dissociation constants (*i.e.*, K_a and K_b , see Table 2). MMP-2 and cdMMP-2 slightly differ only for the interaction parameters α and β (see Table 2), likely reflecting small structural differences referable to the presence or absence of the hemopexin-like domain.

A dampened activity of MMP-2 towards the α -DG (483–628) domain can be achieved by saturating just one of the two binding sites

To functionally discriminate the effect of each binding site, on the basis of the estimated affinity constants of the α -DG (613–651) peptide for the two sites (*i.e.*: $K_a = 3.5(\pm 0.5) \times 10^{-8}$ M and $K_b = 2.1(\pm 0.4) \times 10^{-7}$ M), the inhibition of the α -DG (483–628) domain processing has been compared at two different concentrations of the peptide (*i.e.*, 0.5 μ M and 30 μ M). These experimental conditions ensure that the α -DG (613–651) peptide saturates only the allosteric site at the lowest concentration, whereas both binding sites are occupied at the highest concentration. Fig 7 displays the SDS-PAGE comparative analysis of the α -DG (483–628) domain digestion by MMP-2 over the first 30 minutes, clearly showing that in the absence of inhibitor the 17 kDa band almost disappears ($15 \pm 5\%$ left over) (Fig 7, lane 1 and lane 2). The densitometry analysis shows that the degree of inhibition exerted is very similar (Fig 7, lane 3 and lane 4), despite the two concentrations of the α -DG (613–651) peptide differ by over 50 folds. Within the first 15 minutes of proteolysis, the intensity of the 17 kDa band decreases by only $11 \pm 5\%$ under either low or high α -DG (613–651) peptide concentrations (Fig 7, lane 6 and lane 7, respectively). Thus, the inhibition of MMP-2 occurs even when only the allosteric site, but not the active site, is occupied by the α -DG (613–651) peptide. It clearly confirms that the observed inhibitory effect by the α -DG (613–651) peptide is already exerted through the interaction with the allosteric site even when the MMP-2 active site is available for substrate interaction.

Testing the proteolytic susceptibility of the α -DG (613–651) peptide to MMP-2 by mass spectrometry analysis

Since human α -DG(613–651) peptide is a misfolded sequence of a physiological MMP-2 substrate and one of the sites is able to bind the active site cleft (as indicated by the competitive inhibition behavior, see Fig 4B), we have also evaluated whether MMP-2 can proteolytically digest the α -DG (613–651) peptide. Therefore, we have maximized the chances of proteolysis, not only by prolonging the incubation time (up to 18 hours), but also by increasing both enzyme and peptide concentrations, respectively (*i.e.*, 600 nM MMP-2 and 150 μ M peptide).

LC-MS/MS analysis of α -DG (613–651) peptide, incubated with MMP-2, revealed the presence of new chromatographic peaks after a 5 hours incubation (18.9 min and 23.4 min retention times), not detected in the absence of the enzyme (Fig 8). Such peaks contain fragments

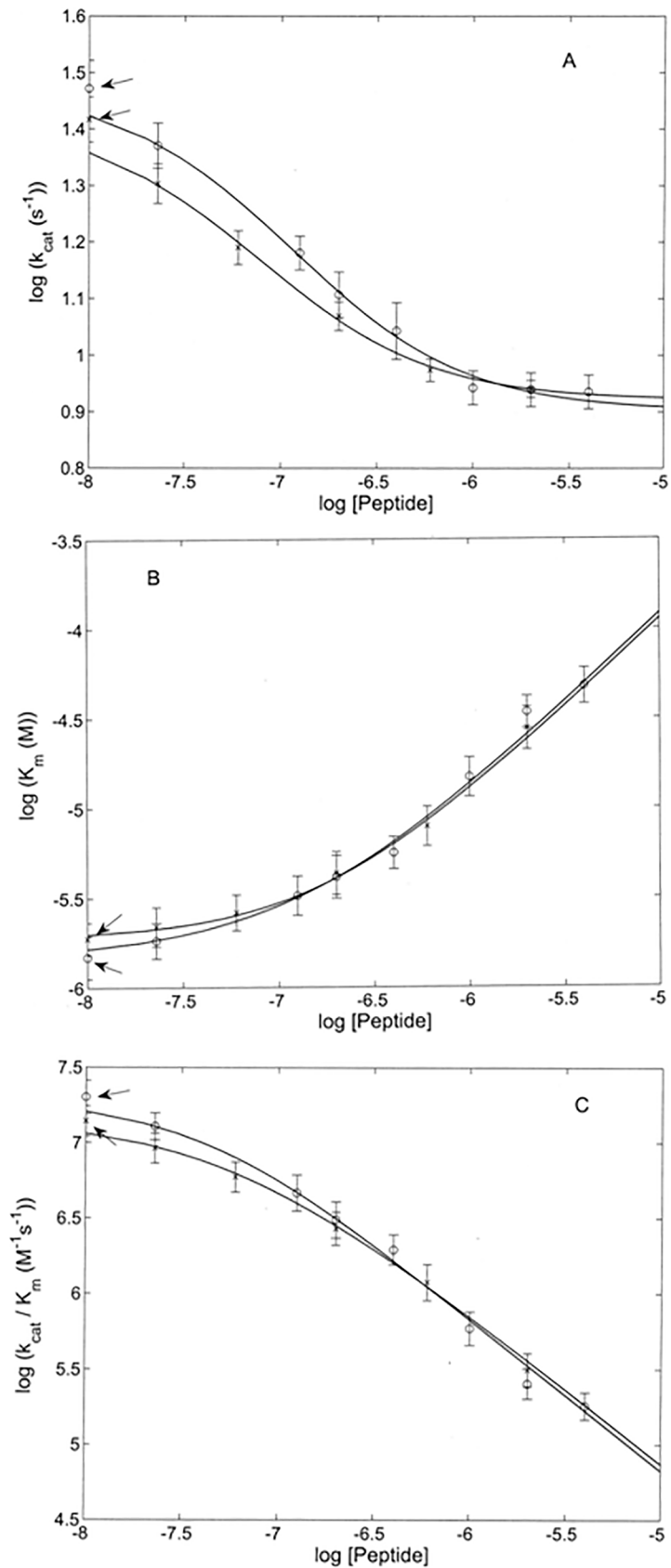


Fig 6. The α DG (613–651) peptide modulation of MMP-2 catalysis. Dependence on the α -DG(613–651) peptide concentration of k_{cat} (panel A), K_m (panel B) and k_{cat}/K_m (panel C) for the enzymatic processing of the fluorogenic peptide by whole MMP-2 (o) and by cdMMP-2 (x) at pH 7.3 and 37°C, as obtained by the analysis of data reported in Figs 4 and 5. Continuous lines have been obtained by applying Eqs (2) and (3), employing parameters reported in Table 1. Arrows indicate the value of the parameter in the absence of the α -DG(613–651) peptide, which is represented as “o” for the intact MMP-2 and as “x” for cdMMP-2.

<https://doi.org/10.1371/journal.pone.0192651.g006>

deriving from the α -DG (613–651) peptide processed by MMP-2. In particular, we identified the sequences (619–629) and (636–651) as the most relevant proteolytic products (Fig 8).

These data showed that α -DG(613–651) peptide can be cleaved by MMP-2, although kinetic experiments indicated that it can allosterically inhibit the MMP-2 enzymatic activity on both α -DG(483–628) domain and the fluorogenic peptide. Altogether, these data suggest that the α -DG (613–651) peptide can be cleaved under extreme conditions, such as very high concentrations of both substrate and enzyme (600 nM MMP-2 active enzyme and 150 μ M α -DG (613–651) peptide) and prolonged incubation time, while the α -DG(613–651) peptide remains essentially stable under conditions employed for all kinetic experiments performed.

Discussion

In a previous paper we have shown that MMP-2 is able to enzymatically process the C-terminal domain (corresponding to residues 483–628) of the murine α -DG, whereas a slightly

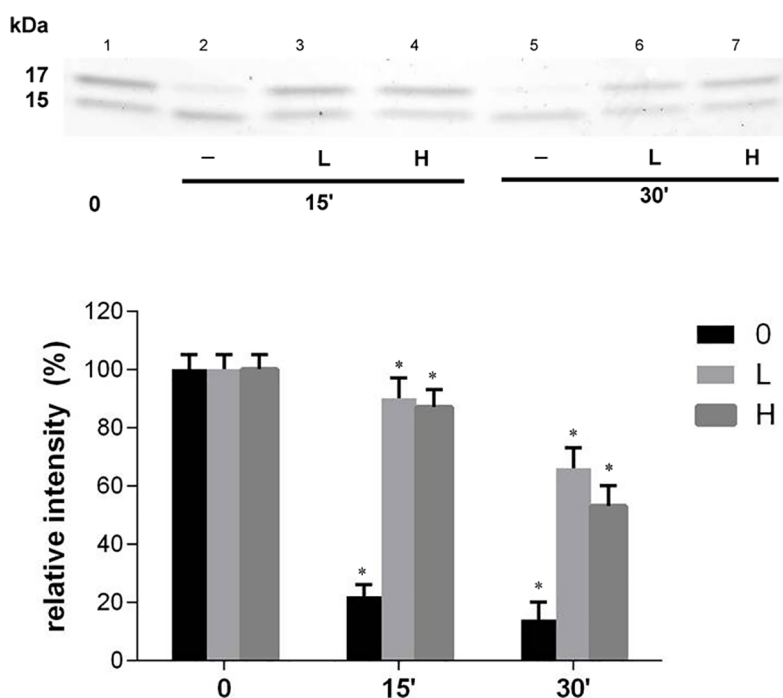


Fig 7. The α DG (613–651) peptide inhibition of the proteolysis of the α DG (483–628) domain by MMP-2. A) SDS-PAGE gel Coomassie blue stained showing the MMP-2 processing of 17 kDa band (α -DG C-terminal domain (483–628)) in the presence of none (0), low (L) and high (H) concentration of the α -DG C-term peptide (615–651) (0.5 and 30 μ M, respectively). A) Three-points time course: time 0 (lane 1), time 15' (lane 2, 3 and 4), time 30' (lane 5, 6 and 7). Control points (0): samples in the absence of α -DG C-term peptide (lane 1, 2 and 5). B) The amounts of intact α -DG (483–628) domain were densitometry quantified; the histograms reported the relative means \pm SD band intensity of the 17 kDa band from three independent experiments. A one-way analysis of variance (ANOVA) was performed and followed by Tukey's honestly significant difference test. (n = 9 for each experimental conditions). (*) represent data significantly different from the respective control (0) at p, 0.05.

<https://doi.org/10.1371/journal.pone.0192651.g007>

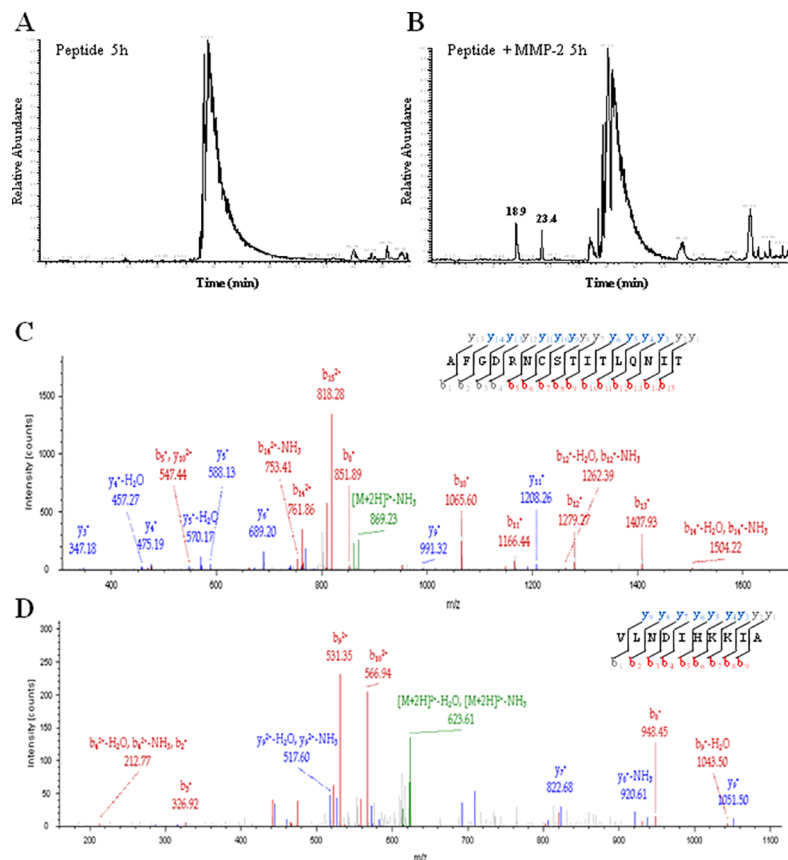


Fig 8. LC-MS/MS analysis of the (613–651) peptide incubated with MMP-2. Chromatographic profiles of the (613–651) peptide incubated for 5 hours without (A) or with (B) MMP-2. MS/MS spectra of the (636–651) peptide eluting at RT 18.9 min (C) and (619–629) peptide eluting at RT 23.4 min (D). Matched b and y ions are colored in red and blue, respectively, while precursor ions losing H₂O or NH₃ are indicated in green.

<https://doi.org/10.1371/journal.pone.0192651.g008>

shortened co-purified fragment (now characterized as α -DG(483–621), see Fig 1) could not be degraded, suggesting that the 621–628 a.a. region is likely to include the sequence recognized by the enzyme [35]. This mechanism finds support in the evidence, obtained in this work, that a synthetic peptide, spanning the amino acids 613–651 of human α -DG (which has a sequence highly homologous to murine DG) and partially overlapping with the C-terminus of murine α -DG (Fig 3), is able to efficiently inhibit the enzymatic activity of MMP-2. Interestingly, the α -DG (613–651) peptide also inhibits the α -DG (483–628) domain proteolysis catalyzed by cdMMP-2, which can occur independently on the presence or not of the 621–628 a.a. region, disrupting both the entire protein construct and its fragmentation product. Therefore, the hemopexin-like domain indeed seems to play a role in substrate recognition, since, when it does not assist the catalytic domain, induces a loss of the interaction specificity, making the enzymatic fragmentation of α -DG(483–621) possible (see Fig 2B, upper panel).

The α -DG(613–651) peptide turned out to be an efficient allosteric inhibitor of MMP-2 even for the proteolysis on a small synthetic fluorogenic substrate, displaying a bimodal behaviour referable to both a non-competitive inhibition (characterized by a higher affinity site with $K_a = 3.5(\pm 0.5) \times 10^{-8} \text{M}$, see Table 2) and a competitive inhibition (characterized by a lower affinity site with $K_b = 2.1(\pm 0.4) \times 10^{-7} \text{M}$, see Table 2). Therefore, based on our kinetic dissection, the peptide appears to have two binding sites on the catalytic domain of MMP-2, a first

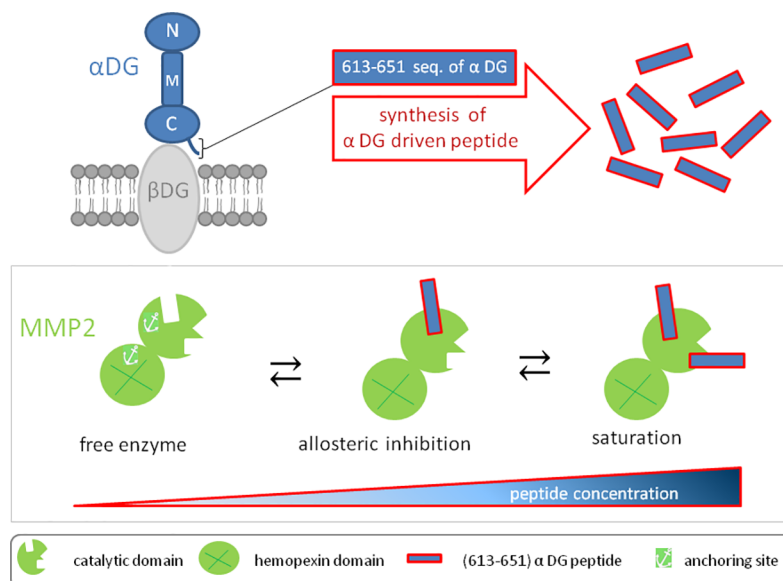


Fig 9. Graphical sketch of the catalytic modulation of MMP-2 by α DG (613–651) peptide. The 613–651 sequence of the human α -DG was used as template to chemically synthesize an MMP-2 inhibitor. This small peptide turned out to modulate the catalysis of human MMP-2 mostly by the two binding sites at the catalytic domain.

<https://doi.org/10.1371/journal.pone.0192651.g009>

one with a higher affinity and topologically distinct from the catalytic site, and a second one, corresponding to the active site and displaying a lower affinity, where the synthetic peptide competes with the substrate. A comparative analysis of the degradation kinetics of the small fluorogenic peptide carried out by cdMMP-2 (where the hemopexin-like domain has been recombinantly removed) in the presence of the α -DG(613–651) peptide revealed that the MMP-2 and cdMMP-2 share both the high and low affinity binding sites for the inhibitory peptide, with very similar dissociation constants, K_a and K_b (see Table 2). The allosteric modulation of MMP proteolytic function exerted by exosites on the surface of the catalytic domain has already been reported for others member of the MMP family [19]. Therefore, it is reasonable to hypothesize that the binding sites are limited to the catalytic domain. However, our data do not allow to rule out the possibility that the α -DG(613–651) peptide also interacts with the hemopexin-like domain of whole MMP-2, interfering with its binding to the 621–628 amino acidic region.

Due to the close similarity between the amino acid sequence of human α -DG(613–651) peptide and that of the murine C-terminal α -DG(483–628) domain, we can envisage a scenario in which it is likely that the whole MMP-2 binds the α -DG(483–628) domain with very high affinity through the hemopexin-like domain. Binding to this first anchoring site (likely shaped by the 621–628 amino acid sequence) allows MMP-2 to direct its proteolytic cleavage activity on a portion of the dystroglycan C-terminal domain comprised between amino acid positions 483 and 621. On the other hand, the absence of this anchoring site (as in the case of the 15 kDa fragment, see Fig 2A (upper lanes) or also in the presence of the α -DG (613–651) peptide) impairs the enzymatic action of MMP-2 on the α -DG (483–628) domain (see Figs 2 and 7).

However, beside this anchoring site for the hemopexin-like domain of MMP-2 on the α -DG 621–628 α -DG domain, an additional site (distinct from the active site) is present in MMP-2, which interacts with the α -DG(483–621) domain. This additional non-competitive site, which is characterized by a high affinity for the α -DG (613–651) peptide, is important for

the substrate recognition also in the absence of the hemopexin-like domain, as indicated by the inhibitory effect elicited by the α -DG (613–651) peptide also on cd-MMP-2 (Fig 2B, lower lanes). This additional site is likely located at the catalytic domain, possibly involving the CBD domain of MMP-2, which predominantly contributes to substrate recognition by MMP-2 [40, 24].

As a whole, in MMP-2 two interactions sites (both distinct from the active site) seem to be operative in the recognition of the α -DG (483–628) domain, one at the hemopexin-like domain and one at the catalytic domain. The α -DG (613–651) peptide seems to be able to efficiently impair their action already at a fairly low concentration; under these circumstances, an allosteric inhibition occurs as the peptide does not prevent the proteolytic action of MMP-2 on additional substrates (e.g. fluorogenic substrate proteolysis, see Figs 4B and 9). This feature, which permits to modulate its inhibitory effect, together with the high kinetic stability of the α -DG(613–651) peptide towards the catalytic activity of MMP-2, makes this dystroglycan-derived synthetic peptide a “lead compound”, which may become a potential template for further pharmaceutical development.

Acknowledgments

This work has been supported by funds from the Italian Space Agency (ASI SMEMCO n. DC-DTE-2011-033 to U.T.).

Author Contributions

Conceptualization: Magda Gioia, Serena Camerini, Marco Crescenzi, Massimo Coletta.

Data curation: Magda Gioia, Diego Sbardella, MariaLuisa Casella, Serena Camerini, Alessandro Gori.

Formal analysis: Magda Gioia, Serena Camerini, Massimo Coletta.

Funding acquisition: Umberto Tarantino, Paola Cozza.

Investigation: Magda Gioia, Giovanni Francesco Fasciglione, Manuela Bozzi.

Methodology: Giovanni Francesco Fasciglione, MariaLuisa Casella, Serena Camerini.

Project administration: Magda Gioia.

Supervision: Magda Gioia, Andrea Brancaccio.

Writing – original draft: Magda Gioia, MariaLuisa Casella, Serena Camerini, Massimo Coletta.

Writing – review & editing: Magda Gioia, Giovanni Francesco Fasciglione, Diego Sbardella, Francesca Sciandra, Marco Crescenzi, Andrea Brancaccio, Massimo Coletta, Manuela Bozzi.

References

1. Ibraghimov-Beskrovnaya O, Ervasti JM, Leveille CJ, Slaughter CA, Sernett SW, and Campbell KP. Primary structure of dystrophin-associated glycoproteins linking dystrophin to the extracellular matrix. *Nature*. 1992; 355: 696–702. <https://doi.org/10.1038/355696a0> PMID: 1741056
2. Barresi R, and Campbell KP. Dystroglycan: from biosynthesis to pathogenesis of human disease. *J Cell Sci*. 2006; 119: 199–207. <https://doi.org/10.1242/jcs.02814> PMID: 16410545
3. Sciandra F, Bozzi M, Bigotti MG, and Brancaccio A. The multiple affinities of α -dystroglycan. *Curr Protein Pept Sci*. 2013; 14: 626–634. PMID: 24206164

4. Akhavan A, Griffith OL, Soroceanu L, Leonoudakis D, Luciani-Torres MG, Daemen A, et al. Loss of cell-surface laminin anchoring promotes tumor growth and is associated with poor clinical outcomes. *Cancer Res.* 2012; 72: 2578–2588. <https://doi.org/10.1158/0008-5472.CAN-11-3732> PMID: 22589276
5. Russo K, Di Stasio E, Macchia G, Rosa G, Brancaccio A, and Petricci TC. Characterization of the β -dystroglycan-growth factor receptor 2(Grb2) interaction. *Biochem Biophys Res Commun.* 2000; 274: 93–98. <https://doi.org/10.1006/bbrc.2000.3103> PMID: 10903901
6. Spence HJ, Chen YJ, Batchelor CL, Higginson JR, Suila H, Carpen O, et al. Ezrin-dependent regulation of the actin cytoskeleton by β dystroglycan Hum. *Mol Genet.* 2004; 13: 1657–1668.
7. Bozzi M, Sciandra F, and Brancaccio A. Role of gelatinases in pathological and physiological processes involving the dystrophin-glycoprotein complex. *Matrix Biol.* 2015; 44–46: 130–137. <https://doi.org/10.1016/j.matbio.2015.02.005> PMID: 25701226
8. Heng S, Paule SG, Li Y, Rombauts LJ, Vollenhoven B, Salamonsen LA, et al. Post-translational removal of α -dystroglycan N terminus by PC5/6 cleavage is important for uterine preparation for embryo implantation in women. *FASEB J.* 2015; 29: 4011–4022. <https://doi.org/10.1096/fj.14-269456> PMID: 26077903
9. Michele DE, Barresi R, Kanagawa M, Saito F, Cohn RD, Satz JS, et al. Post-translational disruption of dystroglycan-ligand interactions in congenital muscular dystrophies. *Nature.* 2002; 418: 417–422. <https://doi.org/10.1038/nature00837> PMID: 12140558
10. Court FA, Zambroni D, Pavoni E, Colombelli C, Baragli C, Figlia G, et al. MMP2-9 cleavage of dystroglycan alters the size and molecular composition of Schwann cell domains. *J Neurosci.* 2011; 31: 12208–12217. <https://doi.org/10.1523/JNEUROSCI.0141-11.2011> PMID: 21865464
11. Losasso C, Di Tommaso F, Sgambato A, Ardito R, Cittadini A, Giardina B, et al. Anomalous dystroglycan in carcinoma cell lines. *FEBS Lett.* 2000; 484: 194–198. PMID: 11078877
12. Sgambato A, Camerini A, Amoroso D, Genovese G, De Luca F, Cecchi M, et al. Expression of dystroglycan correlates with tumor grade and predicts survival in renal cell carcinoma. *Cancer biology & therapy.* 2007; 6: 1840–1846.
13. Kherif S, Lafuma C, Dehaupas M, Lachkar S, Fourier JG, Vrdiere-Sahuque M, et al. Expression of matrix metalloproteinases 2 and 9 in regenerating skeletal muscle: a study in experimentally injured and mdx muscles. *Dev Biol.* 1999; 205: 158–170. <https://doi.org/10.1006/dbio.1998.9107> PMID: 9882504
14. Nadarajah VD, van Putten M, Chaouch A, Garrod P, Straub V, Lochmuller H, et al. Serum matrix metalloproteinase -9 (MMP-9) as biomaker for monitoring disease progression in Duchenne muscular dystrophy (DMD). *Neuromuscul Disord.* 2011; 21: 569–578. <https://doi.org/10.1016/j.nmd.2011.05.011> PMID: 21724396
15. Bozzi M, Sciandra F, Ferri L, Torrerri P, Pavoni E, Petrucci TC, et al. Concerted mutation of Phe residues belonging to the β dystroglycan ectodomain strongly inhibits the interaction with α dystroglycan in vitro. *FEBS J.* 2006; 273: 4929–4943. <https://doi.org/10.1111/j.1742-4658.2006.05492.x> PMID: 17018058
16. Sbardella D, Fasciglione GF, Gioia M, Ciaccio C, Tundo GR, Marini S, et al. Human matrix metalloproteinases: an ubiquitarian class of enzymes involved in several pathological processes. *Mol Aspects Med.* 2012; 33: 119–208. <https://doi.org/10.1016/j.mam.2011.10.015> PMID: 22100792
17. Levin M, Udi Y, Solomonov I, and Sagi I. Next generation matrix metalloproteinase inhibitors—Novel strategies bring new prospects. *Biochim Biophys Acta.* 2017; 1864: 1927–1939. <https://doi.org/10.1016/j.bbamcr.2017.06.009> PMID: 28636874
18. Sternlicht MD, and Werb Z. How matrix metalloproteinases regulate cell behavior. *Annu Rev Cell Dev Biol.* 2001; 17: 463–516. <https://doi.org/10.1146/annurev.cellbio.17.1.463> PMID: 11687497
19. Ratnikov BI, Cieplak P, Gramatikoff K, Pierce J, Eroshkin A, Igarashi Y, et al. Basis for substrate recognition and distinction by matrix metalloproteinases. *Proc Natl Acad Sci USA.* 2014; 111: 4148–4155.
20. Allan JA, Docherty AJ, Barker PJ, Huskisson NS, Reynolds JJ, and Murphy G. Binding of gelatinases A and B to type-I collagen and other matrix components. *Biochem J.* 1995; 309: 299–306. PMID: 7619071
21. Tam EM, Wu YI, Butler GS, Stack MS, and Overall CM. Collagen binding properties of the membrane type-1 matrix metalloproteinase (MT1-MMP) hemopexin C domain. The ectodomain of the 44-kDa autocatalytic product of MT1-MMP inhibits cell invasion by disrupting native type I collagen cleavage. *J Biol Chem.* 2002; 277: 39005–39014. <https://doi.org/10.1074/jbc.M206874200> PMID: 12145314
22. Van den Steen PE, Van Aelst I, Hvidberg V, Piccard H, Fiten P, Jacobsen C, et al. The hemopexin and O-glycosylated domains tune gelatinaseB/MMP9 bioavailability via inhibition and binding to cargo receptors. *J Biol Chem.* 2006; 281: 18626–18637. <https://doi.org/10.1074/jbc.M512308200> PMID: 16672230

23. Gioia M, Fasciglione GF, Marini S, D'Alessio S, De Sanctis G, Diekmann O, et al. Modulation of the catalytic activity of neutrophil collagenase MMP-8 on bovine collagen I. Role of the activation cleavage and of the hemopexin-like domain. *J Biol Chem*. 2002; 277: 23123–23130. <https://doi.org/10.1074/jbc.M110873200> PMID: 11953425
24. Gioia M, Monaco S, van den Steen PE, Sbardella D, Grasso G, Marini S, et al. The collagen binding domain of gelatinase A modulates degradation of collagen IV by gelatinase B. *J Mol Biol*. 2009; 386: 419–434. <https://doi.org/10.1016/j.jmb.2008.12.021> PMID: 19109975
25. Chung L, Dinakarpandian D, Yoshida N, Lauer-Fields JL, Fields GB, Visse R, et al. Collagenase unwinds triple-helical collagen prior to peptide bond hydrolysis. *EMBO J*. 2004; 23: 3020–3030. <https://doi.org/10.1038/sj.emboj.7600318> PMID: 15257288
26. Arnold LH, Butt LE, Prior SH, Read CM, Fields GB, and Pickford AR. The interface between catalytic and hemopexin domains in matrix metalloproteinase-1 conceals a collagen binding exosite. *J Biol Chem*. 2011; 286: 45073–45082. <https://doi.org/10.1074/jbc.M111.285213> PMID: 22030392
27. Rizzo R, Trentini A, Bortolotti D, Manfrinato MC, Rotola A, Castellazzi M, et al. Matrix metalloproteinase-2 (MMP-2) generates soluble HLA-G1 by cell surface proteolytic shedding. *Mol Cell Biochem*. 2013; 381: 243–255. <https://doi.org/10.1007/s11010-013-1708-5> PMID: 23737137
28. Overall CM, and Blobel CP. In search of partners: linking extracellular proteases to substrates. *Nat Rev Mol Cell Biol*. 2007; 8: 245–257. <https://doi.org/10.1038/nrm2120> PMID: 17299501
29. Yamada H, Saito F, Fukuta-Ohi H, Zhong D, Hase A, Arai K, et al. Processing of β -dystroglycan by matrix metalloproteinase disrupts the link between the extracellular matrix and cell membrane via the dystroglycan complex. *Hum Mol Genet*. 2001; 10: 1563–1569. PMID: 11468274
30. Paggi P, De Stefano ME, and Petrucci TC. Synaptic remodelling induced by axotomy of superior cervical ganglion neurons: involvement of metalloproteinase-2. *J Physiol Paris*. 2006; 99: 119–124. <https://doi.org/10.1016/j.jphysparis.2005.12.004> PMID: 16442271
31. Bozzi M, Inzitari R, Sbardella D, Monaco S, Pavoni E, Gioia M, et al. Enzymatic processing of β -dystroglycan recombinant ectodomain by MMP-9: identification of the main cleavage site. *IUBMB Life*. 2009; 61: 1143–1152. <https://doi.org/10.1002/iub.273> PMID: 19946898
32. Sbardella D, Inzitari R, Iavarone F, Gioia M, Marini S, Sciandra F, et al. Enzymatic processing by MMP-2 and MMP-9 of wild-type and mutated mouse β -dystroglycan. *IUBMB Life*. 2012; 64: 988–994. <https://doi.org/10.1002/iub.1095> PMID: 23129308
33. Fukai Y, Ohsawa Y, Ohtsubo H, Nishimatsu SI, Hagiwara H, Noda M, et al. Cleavage of β -dystroglycan occurs in sarcoglycan-deficient skeletal muscle without MMP-2 and MMP-9. *Biochem Biophys Res Commun*. 2017; 492: 199–205. <https://doi.org/10.1016/j.bbrc.2017.08.048> PMID: 28821434
34. Saito F, Saito-Arai Y, Nakamura A, Shimizu T, and Matsumura K. Processing and secretion of the N-terminal domain of α -dystroglycan in cell culture media. *FEBS Lett*. 2008; 582: 439–444. <https://doi.org/10.1016/j.febslet.2008.01.006> PMID: 18201566
35. Sbardella D, Sciandra F, Gioia M, Marini S, Gori A, Giardina B, et al. α -dystroglycan is a potential target of matrix metalloproteinase MMP-2. *Matrix Biol*. 2015; 41: 2–7. <https://doi.org/10.1016/j.matbio.2014.11.007> PMID: 25483986
36. Kazanov MD, Igarashi Y, Eroshkin AM, Cieplak P, Ratnikov B, Zhang Y, et al. Structural determinants of limited proteolysis. *J Proteome Res*. 2011; 10: 3642–3651. <https://doi.org/10.1021/pr200271w> PMID: 21682278
37. De Rosa MC, Pirrollo M, Sciandra F, Giardina B, and Brancaccio A. A second Ig-like domain identified in dystroglycan by molecular modelling and dynamics. *J Mol Graph Model*. 2011; 2: 1015–1024.
38. Gioia M, Fasciglione GF, Monaco S, Iundusi R, Sbardella D, Marini S, et al. pH dependence of the enzymatic processing of collagen I by MMP-1 (fibroblast collagenase), MMP-2 (gelatinase a) and MMP-14 ectodomain. *J Biol Inorg Chem*. 2010; 15: 1219–1232. <https://doi.org/10.1007/s00775-010-0680-8> PMID: 20549272
39. Harrison R, Hitchen PG, Panico M, Morris HR, Mekhaieel D, Pleass RJ, et al. Glycoproteomic characterization of recombinant mouse α -dystroglycan. *Glycobiology* 2012; 22: 662–675. <https://doi.org/10.1093/glycob/cws002> PMID: 22241827
40. Gioia M, Monaco S, Fasciglione GF, Coletti A, Modesti A, Marini S, et al. Characterization of the mechanisms by which gelatinase A, neutrophil collagenase, and membrane-type metalloproteinase MMP-14 recognize collagen I and enzymatically process the two α -chains. *J Mol Biol*. 2007; 368: 1101–1113. <https://doi.org/10.1016/j.jmb.2007.02.076> PMID: 17379243